Oxidation of Metals, Vol. 21, Nos. 1/2, 1983

Morphology of Oxide Scales Formed on Titanium

G. Bertrand,* K. Jarraya,* and J. M. Chaix*

Received February 8, 1983; revised October 25, 1983

High-temperature oxidation of several pure metals and their alloys gives rise to multilayered corrosion scales. This curious morphology has not been the subject of a specific investigation, and its interpretation remains widely open. This paper presents results on titanium foil oxidized in pure oxygen leading to this phenomenon. It analyzes the significant features of the stratification as a function of the main parameters of the reaction kinetics such as temperature, oxygen pressure, oxidation time, and initial thickness of the metallic foil. All the results, including those previously reported, show the importance and the consistency of the studied phenomenon as well as the incapability of providing an unequivocal intepretation at the present time. The analysis of the main results, such as the appearance of a macroscopic order, the existence of boundary limits, and the nonequilibrium state of the structure, shows that a consistent set of data exists to give a meaningful interpretation of multilayered corrosion scales in terms of a nonlinear, far-from-equilibrium organization.

KEY WORDS: titanium oxidation; multilayered scale; nonequilibrium self-organization.

INTRODUCTION

In titanium oxidation studies, scientists have frequently observed an unexpected morphological arrangement of oxidation scales. It consists of a periodical stacking of layers parallel to the reaction interface. Jenkins[1] seems to be the first who reported this result in 1953. The same phenomenon was subsequently confirmed by other investigators, e.g., for oxidations of pure titanium[2–9] and its alloys,[8,10–12] for titanium nitride oxidation[13–15] and also for the reactions of titanium with steam,[16] carbon dioxide,[17] and air.[18] Similar

*Laboratoire de Recherches sur la Réactivité des Solides, Associé au C.N.R.S. (LA. 23), Université de Dijon, BP 138, F 21004 Dijon Cedex, France.

0030-770X/84/0200-0001$03.50/0

multilayered scale structures were observed during oxidation of tantalum[19] and niobium,[20] and during sulfidation of Fe–Cr–Al or Fe–Cr–Al–Mn alloys.[21,22] All these examples are basically different from the periodic precipitations found in internal oxidation of alloys.[23–25]

This curious morphological phenomenon has not been the subject of a specific investigation, and its interpretation remains open. Its understanding should contribute to a better knowledge of the solid-gas reaction mechanisms. This spatial self-organization bears a striking analogy to the dissipative spatial structures resulting from a far-from-equilibrium dynamics.[26] Our recent study of Fe–Cr–Al alloy sulfidation[27] gave decisive arguments for such a link. This paper presents the first results of an identical procedure applied to titanium foils oxidized in pure oxygen. It mainly describes the experimental results and analyzes the significant features of the stratification as a function of the main parameters of the reaction kinetics, such as temperature, oxygen pressure, oxidation time, and initial thickness of the metallic foil. Previous data are considered in our general analysis.

EXPERIMENTAL RESULTS

Material and Procedures

Metal samples were cut from titanium foils of 4, 25, or 250 μm thickness supplied by Alfa-Ventron Co. and had a one side area of about 1 cm^2. Their purity was 99.97% considering only metallic impurities. Crystallographic tests showed a random grain size and orientation. Samples were cleaned in water, acetone, and alcohol, and then dried before exposure to oxygen. Oxidation was performed in pure (99.99%) and dried oxygen in a thermomicrobalance MTB 10-8. The sample was kept in vacuum (10^{-3} torr) at room temperature for about 12 hr before increasing the temperature. After the sample had reached the preset temperature, oxygen was introduced. The temperature and the oxygen pressure ranged from 595 to 965°C and from 100 to 570 torr. Upon completion of the oxidation test the sample was slowly cooled under vacuum. Its cross-section was observed by optical and scanning electron microscopy (SEM); neither mounting nor polishing were done on these sections.

Oxidation Kinetics

We confirm the well-known results that the kinetics curves are made up of two stages. During the first stage, the slope is continuously decreasing; when the second stage is reached, the slope starts increasing, then is constant, and finally decreases. When the temperature is increased, the first stage is shorter and ends at a higher mass gain (Fig. 1a). In one experiment at lower

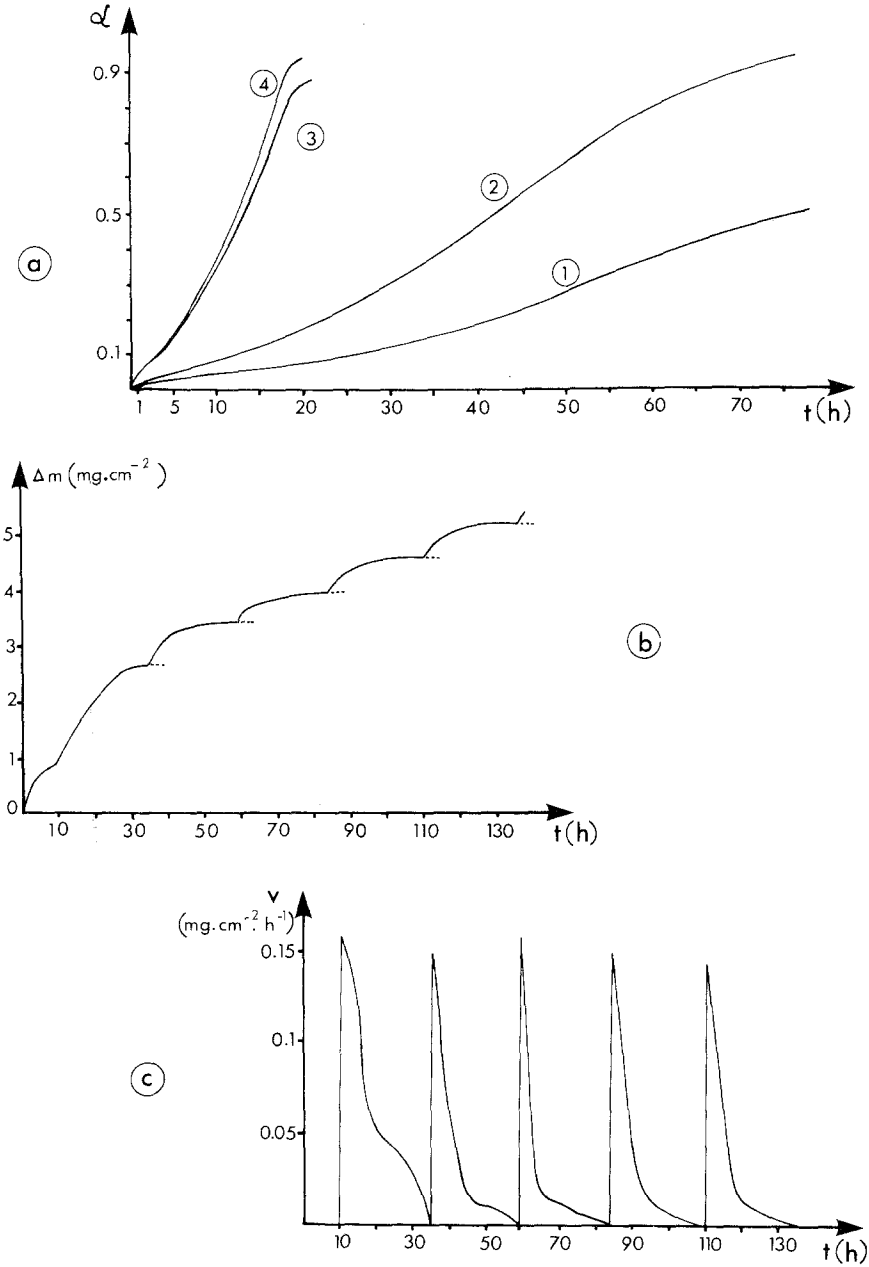

Fig. 1. (a) Kinetic curves $\alpha(t)$ for various experimental conditions, $\alpha(t) = \Delta m_t / \Delta m_\infty$. *1*, $T = 840°C$, $P_{O_2} = 300$ torr; *2*, $T = 840°C$, $P_{O_2} = 500$ torr; *3*, $T = 965°C$, $P_{O_2} = 300$ torr; *4*, $T = 965°C$, $P_{O_2} = 500$ torr. (b) Oscillating mass-gain curve at $T = 695°C$, $P_{O_2} = 105$ torr. (c) Reaction rate vs time (derivative of curve b).

temperature ($T = 695°C$) the kinetics curve is composed of successive parabolic-like parts. The derivative curve, which represents the kinetic rate variations as a function of time, oscillates. During one oscillation a long period of about 25 hr during which the oxidation rate continuously decreases is followed by a very short and steep accelerating period.

Oxidation Time and Morphology

The morphological evolution of the oxide as a function of time is illustrated below for the most favorable conditions ($T = 965°C$, $P_{O_2} = 105$ torr, initial thickness of foil $e_0 = 250\ \mu m$) up to and even after entire oxidation of the sample. (The time for the entire oxidation of the foil is about 15–20 hr.)

Growth of the Oxide Scale

Observations of the sample cross-section by optical microscopy showed three areas. The external oxide appeared bright (yellowish), the intermediate one was black-grey, and the internal one, which was at first the compact residual metallic core, became white after oxidation. Figure 2 illustrates the variation in the mean thickness of each zone as a function of time. First, the thickness of the internal zone decreases quickly, and after 15 hr it remains constant despite the continuing oxidation. Second, the thickness of the

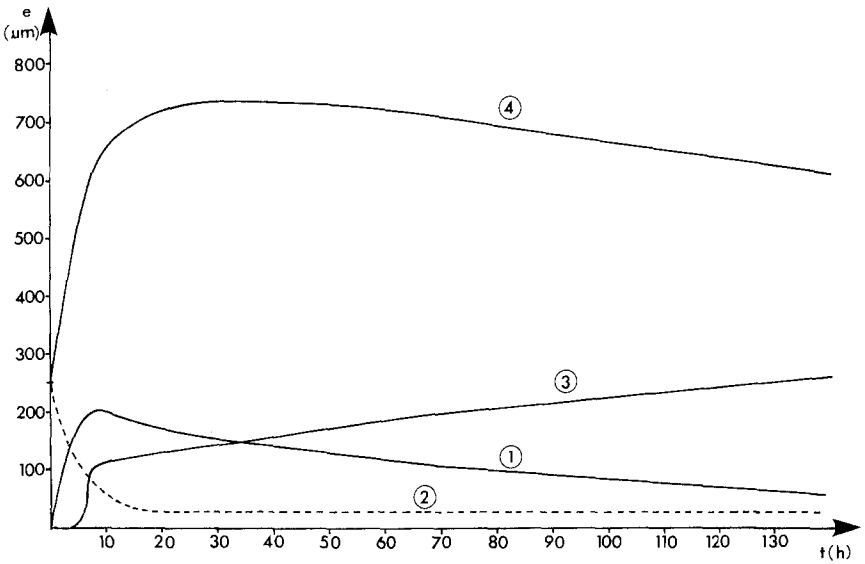

Fig. 2. Variation of the thickness of the different parts of the oxide scale with time. $T = 965°C$, $P_{O_2} = 105$ torr, $e_0 = 250\ \mu m$. *1,* external stratified oxide; *2,* internal; *3,* intermediate; *4,* sample thickness.

external scale first increases and then decreases while the intermediate black-grey area grows. Third, the fully oxidized sample thickness expands from 250 to 700 μm, then it decreases slightly.

The above results were clarified by a SEM examination as illustrated in Fig. 3. Below a superficial thin layer, the external scale is made up of many layers of equal thickness which are parallel with the external surface and are well separated from each other (Fig. 3a, b, e). This scale looks like a "millefeuille" pastry, and as a layer is about 1 μm thick, each external zone contains about 200 layers when its maximum thickness is reached. The morphology of the internal oxide is very different. It is not stratified but coarse grain crystallized (Fig. 3d, f). The intermediate scale, where the oxide is compact (Fig. 3g), grows progressively from the internal interface consuming the stratified zone, which disappears almost completely (Fig. 3c, d). The bulk of the three oxide zones was composed only of rutile as shown by X-ray diffraction analysis. Nevertheless the color revealed that internal and external zones were made up of stoichiometric rutile whereas the intermediate one recrystallized into a nonstoichiometric oxide.

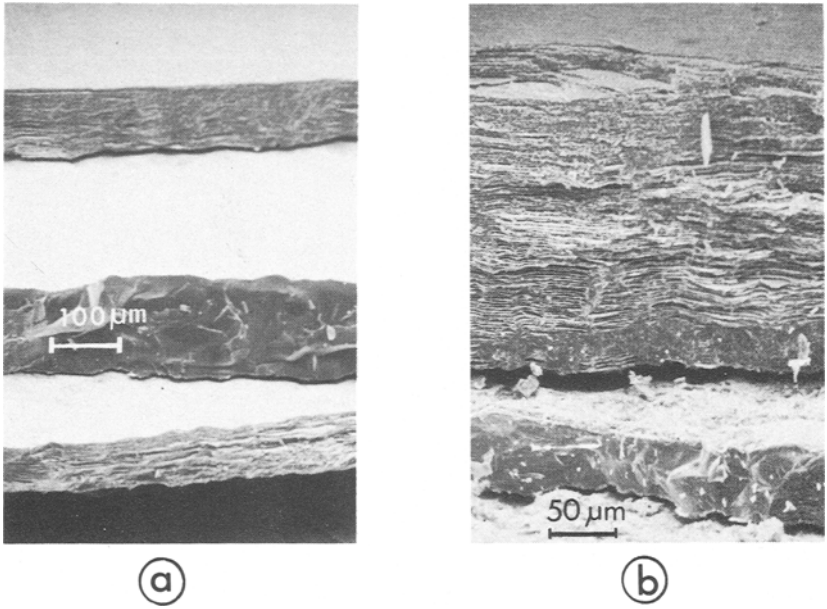

Fig. 3. SEM examination of cross-sections of the sample after different reaction periods at $T = 965°C$, $P_{O_2} = 105$ torr, and $e_0 = 250$ μm. (a) $t = 3$ hr, (b) $t = 7$ hr, (c) $t = 140$ hr, and (d) $t = 7$ hr show the internal, the external, and the intermediate zones; (e) $t = 7$ hr shows the stratified oxide; (f) $t = 70$ hr shows the internal oxide; (g) $t = 70$ hr shows the intermediate recrystallized oxide.

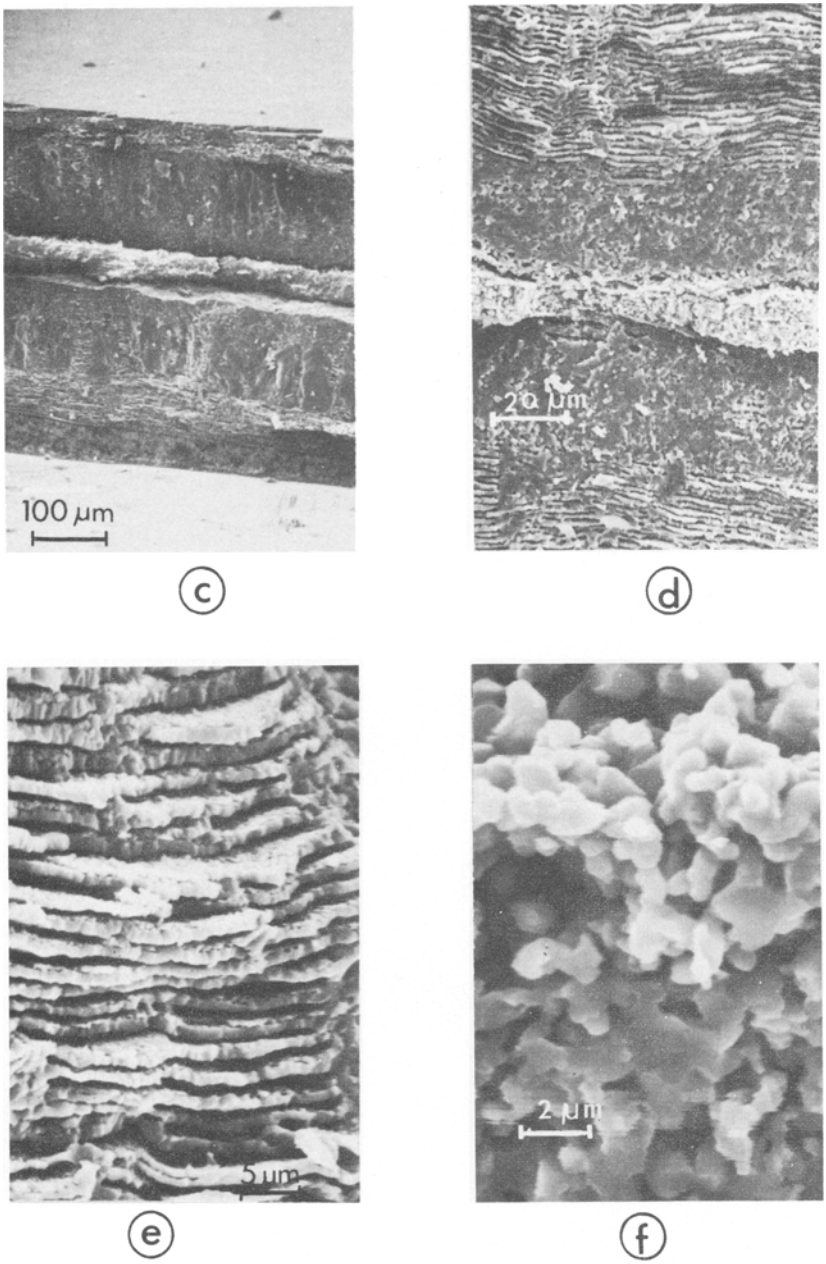

Fig. 3. Continued.

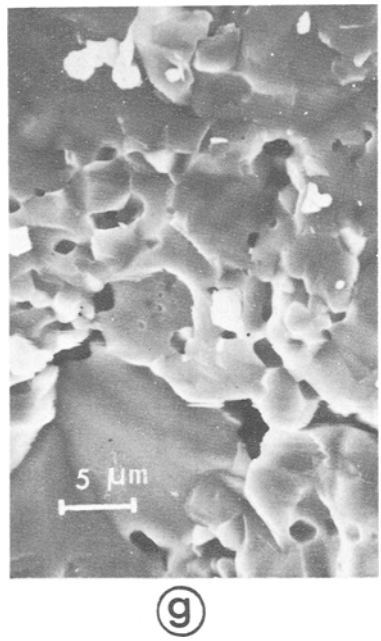

Fig. 3. Continued.

Morphology of a Layer

The layer morphology changes with time, as shown in Fig. 4. At the beginning a layer is constituted by a flat coarse-grained frame with a sprinkle of numerous small grains (Fig. 4a). Then, following a growth process (Fig. 4a–d) only one layer of big grains placed side by side or joined together remains (Fig. 4e). A few grains act as bridges between two layers allowing for their coalescence. Thus, two successive steps occur during the complete oxidation process of the sample. The first is the growth of a multilayered scale of stoichiometric rutile, the second is its recrystallization to form a compact nonstoichiometric protective scale.

Influence of Thermodynamic Parameters

Two parameters will be considered: the furnace temperature and the oxygen pressure.

Furnace Temperature ($P_{O_2} = 105$ torr, $e_0 = 250\ \mu$m)

Below 630°C no significant mass grain has been recorded after 360 hr exposure. Figures 5(a, b, c) and 6 illustrate the influence of temperature on the morphology of the oxide scale. The mean thickness of a layer decreases when the temperature increases. However, two opposite effects must be

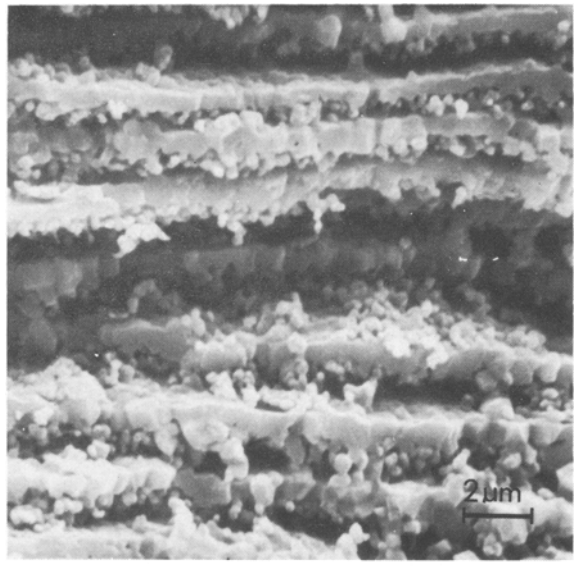

(a)

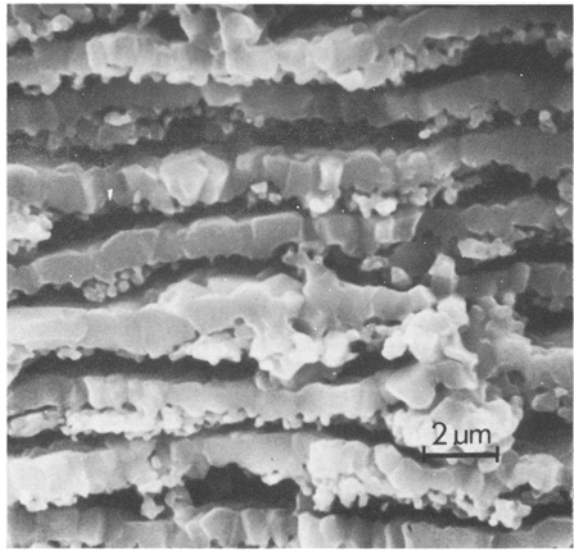

(b)

Fig. 4. Evolution of layer morphology vs time at $T = 965°C$, $P_{O_2} = 105$ torr, $e_0 = 250\ \mu m$. (a) $t = 3$ hr; (b) $t = 7$ hr; (c) $t = 15$ hr; (d) $t = 70$ hr; (e) $t = 140$ hr.

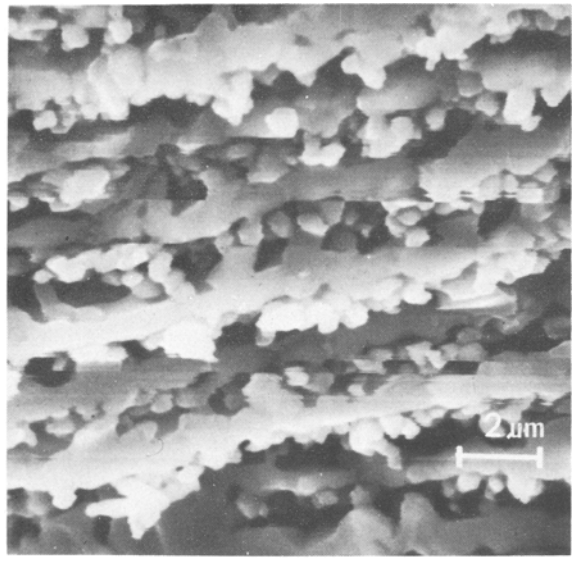

(c)

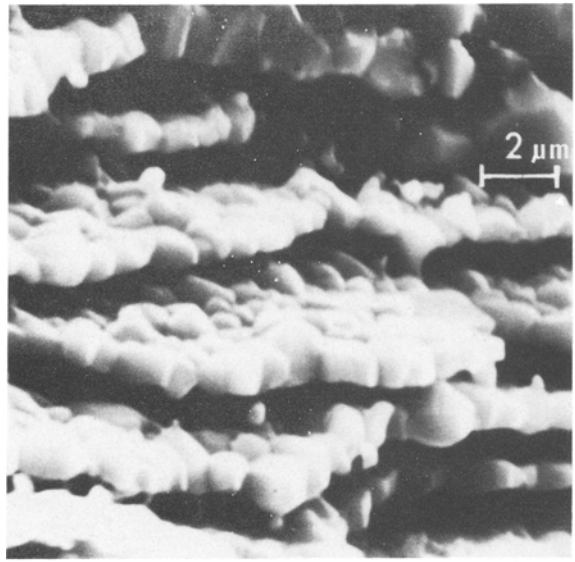

(d)

Fig. 4. Continued.

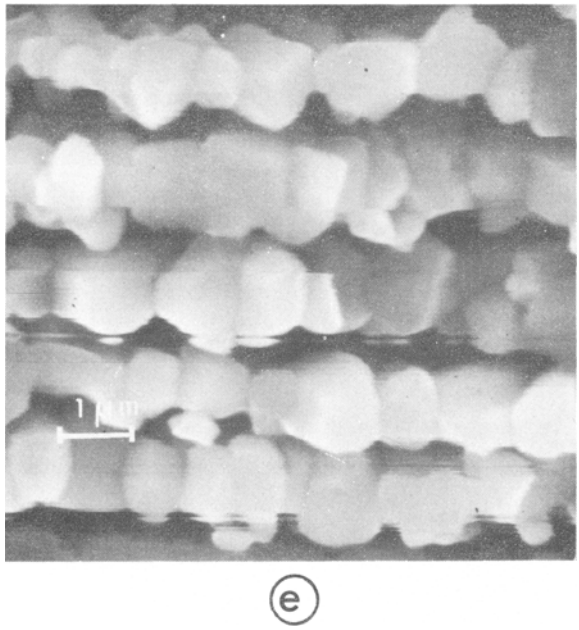

Fig. 4. Continued.

considered. On the one hand, the rutile layer thickness decreases strongly; on the other hand, the spacing between two layers widens from a thin crack of about 0.1 μm at 800°C to a furrow becoming larger than the rutile layer at 1100°C according to Coddet's results.[8]

Oxygen Pressure ($T = 965$°C, $e_0 = 250$ m)

As can be seen in Fig. 5(d, e, f), the effect of oxygen pressure on the general morphological features is negligible. The mean thickness of a layer remains almost constant, but the structure of each layer just appears slightly different: the crystallites become smaller and smaller, and their number increases with the oxygen pressure.

Initial Thickness of the Sample

The sample thickness ($T = 965$°C, $P_{O_2} = 105$ torr) may be affecting the oxidation kinetics. To test such an effect, foils of different initial thicknesses, e_0, were studied. For $e_0 \geq 25$ μm, the multilayered scale was observed (Fig. 5, Fig. 7c). When the titanium foil was 4 μm thick, the observation was different: only two zones appeared, an external one on both sides and an internal one (Fig. 7a, d); each of these was made up of numerous small

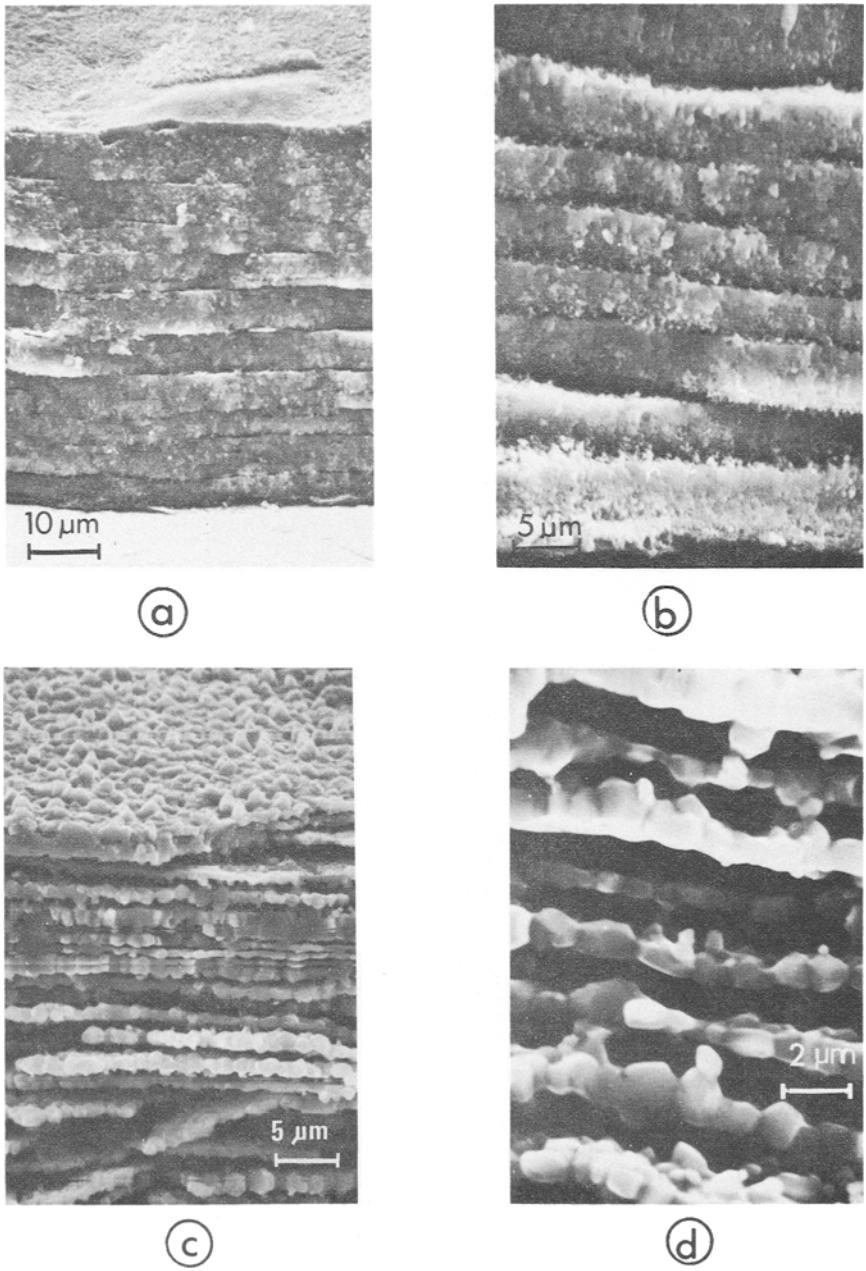

Fig. 5. Variation of the stratification vs temperature or oxygen pressure. At $P_{O_2} = 105$ torr: (a) $T = 790°C$, $t = 24$ hr; (b) $T = 840°C$, $t = 70$ hr; (c) $T = 965°C$, $t = 70$ hr. At $T = 965°C$: (d) $P_{O_2} = 105$ torr, $t = 27$ hr; (e) $P_{O_2} = 300$ torr, $t = 25$ hr. (f) $P_{O_2} = 570$ torr, $t = 25$ hr.

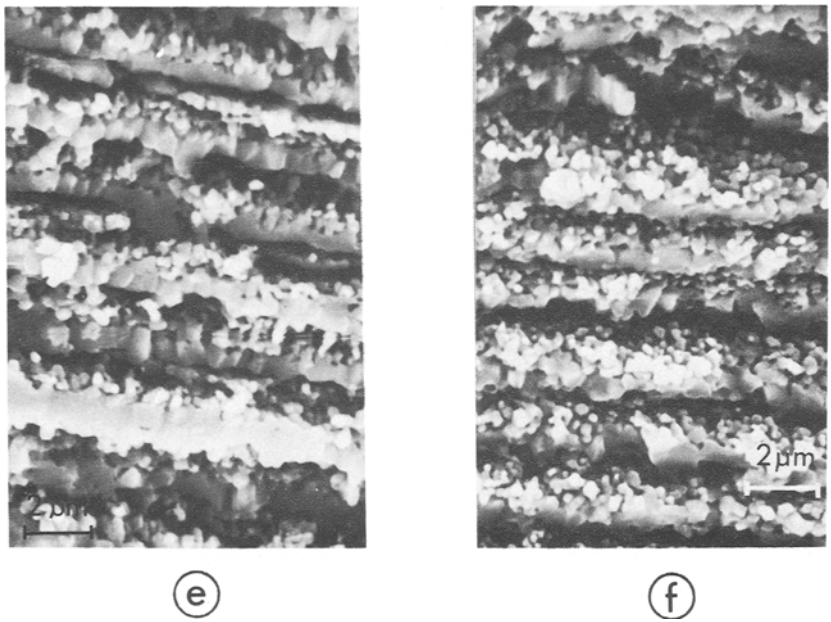

Fig. 5. Continued.

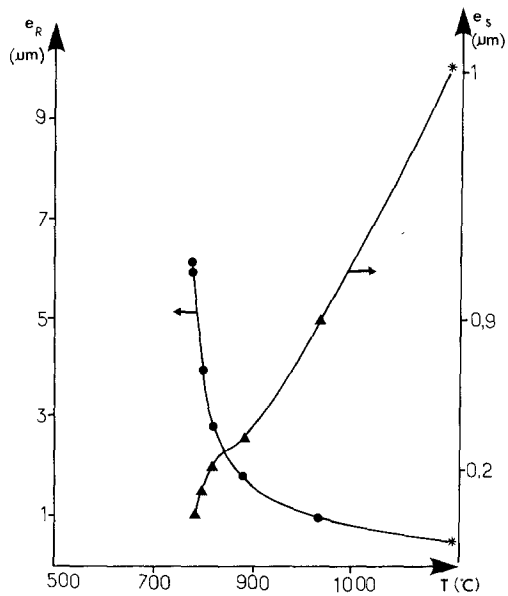

Fig. 6. Layer thickness variation vs temperature. *1*, rutile layer, e_R (● this work; *Coddet[8]). *2*, interlayer spacing, e_S (▲).

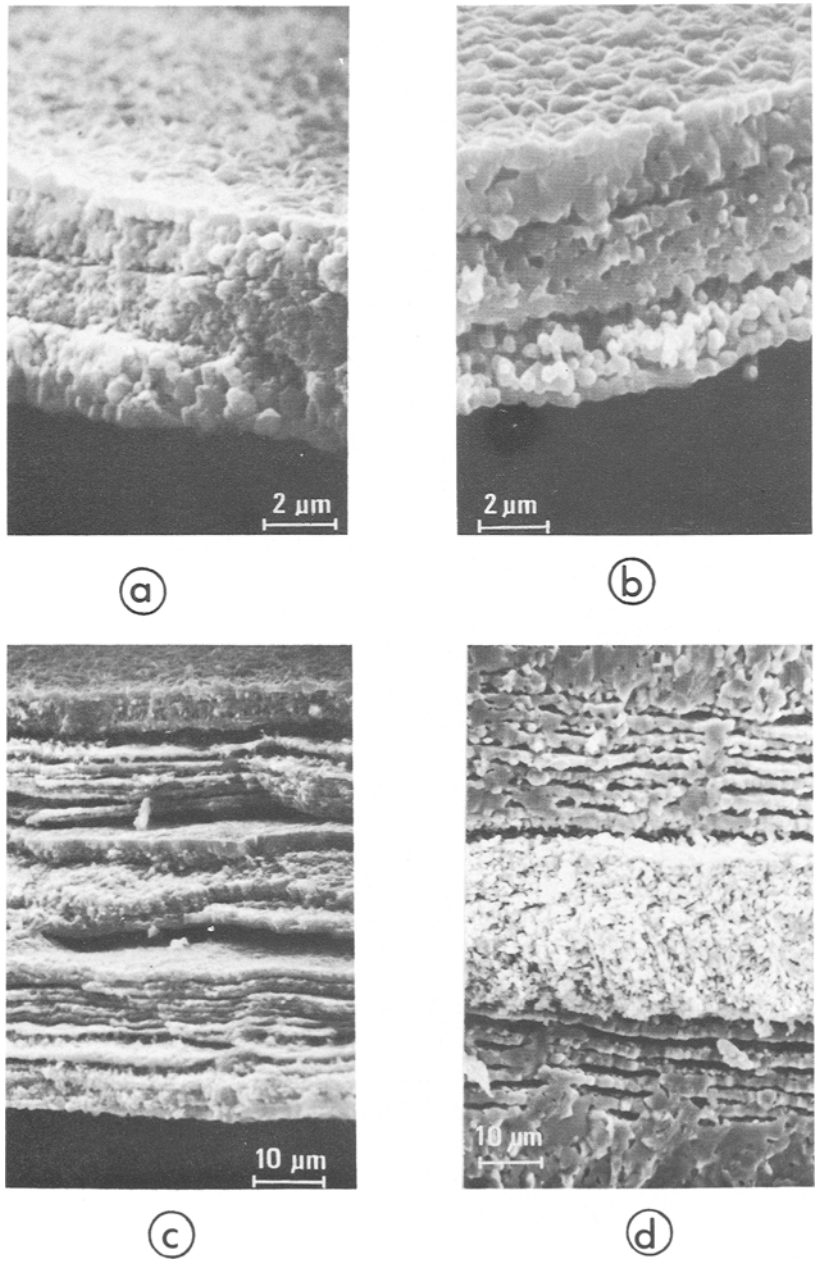

Fig. 7. Influence of initial sample thickness, e_0, on stratification. (a) $e_0 = 4\ \mu$m, $t = 1$ hr; (b) $e_0 = 4\ \mu$m, $t = 5$ hr; (c) $e_0 = 25\ \mu$m, $t = 1$ hr; (d) $e_0 = 250\ \mu$m, $t = 27$ hr (note: the internal oxide is not stratified).

grains randomly distributed and recrystallized at different rates. The absence of stratification was also noticed when the oxidized internal part of the thick samples was observed (Fig. 7d).

Before discussing the experimental results, it should be stressed that recrystallization, which is shown on most micrographs, is an important phenomenon which could make the observed oxide different from what it was at its formation. The morphologies are not "quenched in" after the passage of the reaction front, and the stratification fits into a complex morphological dynamics. The temperature, oxygen pressure, sample size and geometry, and time of thermal treatment are relevant parameters of the formation, maintenance, and disappearance of the different morphologies.

DISCUSSION

State of the Art

No chemical mechanism can explain at the present the formation of periodic multilayered corrosion scales. No model exists to predict it. All the same, some ideas have been put forward, but they are not based on quantitative considerations. The most frequent explanation for such scales is based on the high value of the Pilling and Bedworth ratio (PBR) between rutile and titanium (PBR = 1.75)[28]; compressive stresses in oxide and tensile stresses in metal are assumed to develop at the metal/oxide interface. These stresses increase until a bearable maximum value is reached, which corresponds to a critical thickness at which the scale breaks. The access of oxygen to a fresh metallic surface is then easy. The process repeats itself and results in the stratified morphology of the oxide. We should point out that the observation of this morphology is not specific to reactions where PBR $>$ 1, since a stratified scale is also found during oxidation of pyrite to hematite.[29]

Another hypothesis assumes that the stratification is the consequence of exfoliation in the metal owing to diffusion of oxygen.[3,30] Accordingly, a great variation in the lattice parameters appears in the Ti-O solid solution at 25.9 at.% of oxygen. Stress buildup at this composition leads as above to a detachment of a layer of critical thickness of the solid solution. This would be followed by a fast oxidation of this distinctive layer.

A third approach is to consider that the scale is built-up essentially by cationic diffusion, which implies production of metal vacancies at the metal/oxide interface.[5,18] The clustering of these interfacial vacancies, at a definite amount of them, would cause the periodic stripping of the metallic surface.

Finally, the cooling of the sample may be put forward as an explanation. The internal morphology of scales is always observed at room temperature

after cooling in the reaction chamber. This cooling period could generate some transformations of the corrosion scale morphology. Although this approach remains open to discussion, it should be mentioned that *in situ* cracking during oxidation has been detected by acoustic emission.[31] Moreover, on the one hand, the variation of the layer thickness as a function of the reaction temperature, and on the other hand, the processes of recrystallization and growth as a function of time are arguments proving the appearance of layers during the reaction itself. If it is true that the random cracks observed in several micrographs probably result from cooling, this does not explain the repeating morphological order[19] and, in some cases, the chemical order of the oxidized scale.

The lack of quantitative data about adhesion, cracking, diffusion under stresses, etc., under experimental conditions prevents a test of the first three explanations. The existence of a critical value of the oxide scale thickness may only be supposed since no criterion has so far been defined.

Remarkable Experimental Occurrences

As indicated, the stratification has been observed by numerous scientists in various oxidation reactions. When only considering titanium oxidation a good consistency of the results is found. Figure 8 summarizes the published variations of layer thickness with temperature[6–9,15,17]; the experimental

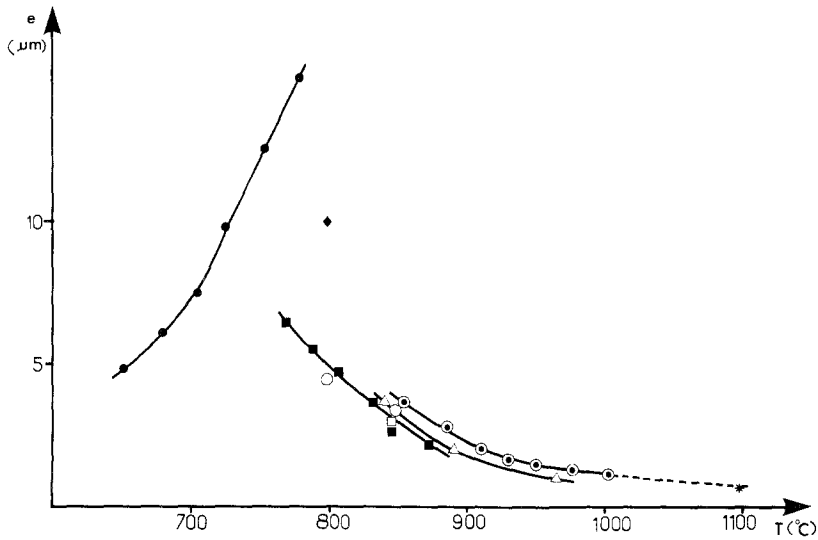

Fig. 8. Variation of thickness vs temperature. Titanium sheets oxidized in pure oxygen: ■ Lefort *et al.*[9]; △ this work; □ Feldman *et al.*[7]; *Coddet[8]; ○ Garcia *et al.*[6]. Titanium nitride oxidized in pure oxygen: ⊙ Desmaison *et al.*[15] Titanium sheets oxidized in CO_2: ● Desmaison.[17] Titanium sheets oxidized in water vapor: ◆ Coddet.[8]

results are located on a mean curve if the oxidant is oxygen. Other oxidant gas (i.e., CO_2) modifies markedly the corrosion layer thickness and its variation with temperature. It should be noted that although the origin and the purity of the titanium sheets used in these experiments varied, the consistency of the results is satisfactory.

Correlations between stratification and oxidation kinetics have been considered[6,10,14,15]: in some cases a careful study of the kinetics curves shows that they are made up of pseudoparabolic parts, each corresponding approximately to the same specific mass gain. Figure 1b shows such an oscillating kinetics curve obtained experimentally. Such curves can only be observed if the breaking occurs simultaneously along the whole metal/oxide interface; otherwise no periodicity will be observed on the kinetics curves.

The oxide does not always appear stratified. The multilayered morphology seems to occur more readily at higher temperature. Thus, during oxidation of titanium nitride powder $TiN_{0.95}$,[13] the oxide scale looked unlayered when the reaction occurred at a temperature below 830°C and multilayered above it. Titanium sheets oxidized in water vapor[8] at low pressure showed a transition from monolayer to multilayer at about 1000°C. The TU12 alloy oxidation studies[8] lead to the same conclusion.

Pressure variation can also cause some morphological changes. During titanium oxidation at 400 torr in pure oxygen at 1100°C, an unstratified rutile scale was obtained,[8] whereas a stratified one was obtained at the same temperature at 1 torr in pure oxygen. In the case of oxidation of $TiN_{0.79}$ nitride sheets at 1095°C[15] the scale stratified above 60 torr but became spongy below it. Finally, increasing temperature often leads to the disappearance of stratification and the formation of a compact scale. Nevertheless it is difficult to distinguish whether this fact results from a formation without layers or from a very quick recrystallization which homogenizes almost immediately the lamellar scale.

All these results show the importance and the compatibility of the studied phenomenon and, despite everything, the inability to give an indisputable interpretation. All the results can be gathered in a very coherent and attractive framework by illustrating this phenomenon as a new example of dissipative structures, as will be shown below.

A New Conceptual Framework for Three Types of Results

Macroscopic Order Appearance

What is unexpected is the repetitive organization of layers parallel to interfaces. Generally corrosion scales do not reveal this regular order. Only one scale with randomly distributed crystallites and uniform chemical composition is generally observed. Different successive phases can also

form but without repetition (duplex scales, etc.). The more or less large affinity of metallic elements for the oxidant or the varied degrees of oxidation of the element[32] accounts for this arrangement, which is also directly related to the geometry of the initial solid-gas system. On the contrary, the spatial self-organization in multilayered oxides reveals a symmetry breaking along the growth axis of the scale. As seen, e.g., in Fig. 1, this order can result from a temporal periodical phenomenon at the reaction interface. Such a periodical growth rate produces a macroscopic morphological order.

Existence of Boundary Limits

The corrosion scale layering arises only within definite boundary limits of some parameters (see above). Outside these limits, the scale shows an unstratified structure as expected. The variation of reaction parameters setting the distance from equilibrium, such as furnace temperature, gas pressure and composition, and solid-phase composition of alloy, reveals the boundary limits which separate the field of the homogeneous scale from that of a stratified scale. We also found that the initial thickness of the metallic sample must be sufficient to give rise to a stratification (see above). This result suggests the existence of a critical initial thickness, and consequently, the "size" of the system is one of the parameters of appearance of stratification.

Nonequilibrium of the Structure

The disappearance of the layers with the holding time of the sample in the furnace shows that the structured state of the scale (cf. Figs. 2 and 3c, d, g) is not its equilibrium state. Transport of matter associated with the recrystallization which occurs after stratification (Fig. 4) is an essential indication of the nonequilibrium state of the stratified scale. Subsequent processes result in themodynamic equilibrium and make the corrosion scale homogeneous. The persistence of layers at low temperature can be attributed to the quenching of an unstable state. This spatial macroscopic organization of the matter must be clearly distinguished from that which results from equilibrium crystallographic order. It is formed by irreversible fluxes, like chemical reactions, diffusion, stresses, etc.

CONCLUSIONS

Based on analysis of the available data it emerges that the ordered morphology of the corrosion scale is typical of a nonequilibrium ordering. Such a periodic kinetics regime should not be confused with the classical steady-state regime, which is unstable (unobserved) in these conditions. Instability of the steady-state regime occurs only if the critical boundary

limit (bifurcation point) of some parameters, setting a definite distance from equilibrium, is crossed.

The present approach only sets a framework, which is nevertheless important because it directs the search for the explanation of stratified scales towards research on the instability of the steady-state growth regime. It does not give a detailed interpretation of the reaction mechanism; in particular, it does not point out the nonlinear processes which cause the breaking of the stability of the steady homogeneous state. For titanium oxidation, further quantitative experimental studies are needed before any adequate model can be implied.

In order to show the relevance of such an approach, we elaborated on a theoretical study[33] of a reaction mechanism, which is classical in corrosion, but without a-priori steady and rate-limiting step approximations. Such an analysis leads to relevant results for nonsteady-state behavior. In particular, it predicts the existence of a critical thickness of the corrosion scale and the possibility of a periodic growth.

REFERENCES

1. A. E. Jenkins, *J. Inst. Met.* **82**, 213 (1953–54).
2. P. Kofstad, K. Hauffe, and H. Kjöllesdal, *Acta. Chem. Scand.* **12**, 239 (1958).
3. G. R. Wallwork and A. E. Jenkins, *J. Electrochem. Soc.* **106**, 10 (1959).
4. J. Stringer, *Acta Met.* **8**, 758 (1960).
5. T. Hurlen, *J. Inst. Met.* **89**, 128 (1960–61).
6. E. A. Garcia, X. Lucas, G. Beranger, and P. Lacombe, *C.R. Acad. Sci. Paris*, Série C, **278**, 827 (1974). E. A. Garcia, *Met. Corros. Ind.* **638**, 319 (1978); **639–640**, 355 (1978).
7. R. Feldman, M. Dechamps, and P. Lehr, *Met. Corros. Ind.* **617**, 1 (1977); **619**, 105 (1977); **620**, 140 (1977). M. Feldman and P. Lehr, *J. Less-Common Metals*, **56**, 193 (1977).
8. C. Coddet, doctoral thesis, I.N.P. Grenoble (1977).
9. P. Lefort, J. Desmaison, and M. Billy, *C.R. Acad. Sci. Paris*, Série C, **286**, 361 (1978).
10. P. Sarrazin and C. Coddet, *Corros. Sci.* **14**, 83 (1974); C. Coddet, P. Sarrazin, and J. Besson, *J. Less-Common Met.* **51**, 1 (1977).
11. R. F. Voitovich, E. I. Golovko, and L. V. D'Yakonova, *Zash. Met.* **12**, 590 (1976).
12. H. Becker, *Z. Metallkde.* **72**, 679 (1981).
13. P. Lefort, J. Desmaison, and M. Billy, *C.R. Acad. Sci. Paris*, Série C, **285**, 361 (1977).
14. P. Lefort, J. Desmaison, and M. Billy, *J. Less-Common Met.* **60**, 11 (1978).
15. J. Desmaison, P. Lefort, and M. Billy, *Oxid. Met.* **13**, 203 (1979).
16. P. Sarrazin, F. Motte, J. Besson, and C. Coddet, *J. Less-Common Met.* **59**, 111 (1978).
17. M. Desmaison, doctoral thesis, Limoges (1981).
18. R. F. Voitovich, E. I. Golovko, and L. V. D'Yakonova, *Russ. J. Phys. Chem.* **49**, 683 (1975).
19. J. Stringer, *J. Less-Common Met.* **16**, 55 (1968).
20. J. A. Roberson and R. A. Rapp, *Trans. TMS-AIME*, **239**, 1327 (1967).
21. Y. Morel, J. P. Larpin, and M. Lambertin, *Ann. Chim. Fr.* **4**, 25 (1979).
22. J. Lions, J. P. Trottier, and M. Foucalt, *Mém. Et. Sci., Rev. Metall.*, 743 (1980).
23. R. A. Rapp, *Acta Met.* **9**, 730 (1961).
24. Y. S. Shen, E. J. Zdanuk, and R. H. Krock, *Met. Trans.* **2**, 2839 (1971).
25. V. A. Van Rooijen, E. W. Van Royen, J. Vrijen, and S. Radelaar, *Acta Met.* **23**, 987 (1975).
26. P. Glansdorff and I. Prigogine, *Thermodynamic Theory of Structure, Stability and Fluctuations* (Wiley, New York, 1974); G. Nicolis and I. Prigogine, *Self-Organization in Non-Equilibrium Systems* (Wiley, New York, 1977).

27. G. Bertrand, J. M. Chaix, and J. P. Larpin, *Mat. Res. Bull.* **17**, 69 (1982).
28. C. Béranger and C. Coddet, *J. Microscop. Spectrosc. Electron.* **5**, 793 (1980).
29. F. R. A. Jorgensen and F. J. Moyle, *Met. Trans. B*, **12B**, 769 (1981).
30. P. Kofstad, P. B. Anderson, and O. J. Krudtaa, *J. Less-Common Met.* **3**, 89 (1961).
31. C. Coddet, J. F. Chretien, and C. Beranger, *C.R. Acad. Sci., Paris*, Série C, **282**, 815 (1976).
32. G. Romeo, W. W. Smeltzer, and J. S. Kirkaldy, *Chim. l'Industria*, **54**, 28 (1972); *J. Electrochem. Soc.* **118**, 1336 (1971); B. D. Lichter and C. Wagner, *J. Electrochem. Soc.* **107**, 168 (1960); J. S. Kirkaldy, G. M. Bolze, C. Mccutcheow, and D. J. Young, *Met. Trans.* **4**, 1519 (1973); J. Benard, *L'Oxydation des Métaux* (Gauthier Villars, Paris, 1962); G. J. Yurek, J. P. Hirth, and R. A. Rapp, *Oxid. Met.* **8**, 265 (1974); A. T. Fromhold Jr., *J. Chem. Phys.* **74**, 6525 (1981).
33. J. M. Chaix, M. Hennenberg, and G. Bertrand, *J. Chim. Phys.* **79**, 781, 791 (1982).